Flexible Multimode Endoscope for Tissue Reflectance and Autofluorescence Hyperspectral Imaging

Neil T. Clancy*[1,2], Julian Teare[2], George B. Hanna[2], Daniel S. Elson[1,2]
Hamlyn Centre for Robotic Surgery, Institute of Global Health Innovation, Imperial College London, SW7 2AZ, UK;
Department of Surgery and Cancer, Imperial College London, SW7 2AZ, UK.
**n.clancy@imperial.ac.uk*

Abstract: A dual reflectance and autofluorescence spectral imaging probe compatible with the biopsy channels of standard flexible endoscopes is demonstrated. Spatially-resolved haemoglobin and autofluorescent signals from porcine bowel were obtained *in vivo*.
OCIS codes: (170.2150) Endoscopic imaging; (170.6280) Spectroscopy, fluorescence and luminescence; (110.4234) Multispectral and hyperspectral imaging.

1. Introduction

Polyps discovered during colonoscopy are routinely removed despite many being ultimately confirmed to be non-neoplastic (~40% [1]) and of no risk to the patient. A means of objectively classifying polyps *in situ* would allow clinicians to leave non-neoplastic tissue in place, reduce risk of polypectomy injury and save the hospital histology costs. Furthermore previous studies have shown that biopsy techniques used in upper GI endoscopy to diagnose Barrett's oesophagus are subject to sampling error and false negatives [2]. Quantitative assessment of the tissue properties during inspection would enable the clinician to optimise biopsy location and reduce the false negative rate.

Work using commercial systems, such as narrowband imaging (NBI), has shown potential in identifying Barrett's oesophagus and classifying colonic polyps. However reported improvements are often variable and not statistically significantly better than white light assessment alone [3]. These techniques also still rely on the clinician to interpret the images and thus, are subject to the experience and training level of that individual. Research systems using dual wavelength excitation of endogenous fluorophores in the respiratory chain have reported signal changes specific to neoplastic and non-neoplastic tissue [4]. Additionally quantitative spectral imaging has shown that measurement of the tissue's optical properties yields functional and structural information relevant to pathology [5, 6].

In this paper a multimodal endoscopic imaging probe is proposed to collect hyperspectral and dual-excitation autofluorescence data from tissue. This will provide high resolution spectral data for use with computational classifiers that commercial systems such as NBI are incapable of acquiring. A flexible probe, compatible with endoscopic biopsy channels, is proposed to relay excitation and emitted/reflected light between the tissue surface and the spectral detection hardware since current standard endoscopes use tip-mounted camera chips. The system hardware is outlined and characterised, and a demonstration of its usability in an *in vivo* procedure is presented.

2. Materials and Methods

Figure 1 shows the probe coupled to reflectance and autofluorescence hyperspectral imaging (HSI) optics.

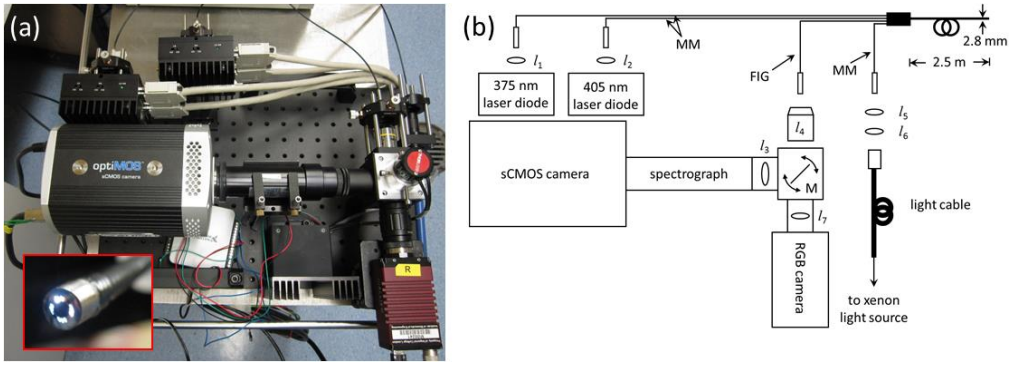

Fig. 1. (a) Photograph of the experimental set-up. Inset: probe tip. (b) System schematic showing the imaging probe and its constituent fibre image guide (FIG) and multimode (MM) illumination fibres. Lenses, denoted '*l*', have focal lengths as follows: l_1, l_2 = 10 mm, l_3 = 100 mm, l_4 = 10× objective, l_5 = 10 mm, l_6 = 35 mm, l_7 = 50 mm. The light cable is an optical fibre bundle carrying light from the xenon light source to the fibre probe. The distal end of the probe is 2.8 mm in diameter.

The custom-designed probe (FiberTech Optica, Inc., Canada) incorporates a 30,000-element fibre image guide (FIG; Fujikura Ltd., Japan) with a tip-mounted GRIN imaging lens (Grintech GmbH, Germany). This is surrounded

by 21 multimode optical fibres, divided into three arms, coupled to a xenon lamp (Karl STORZ GmbH, Germany), 375 nm laser (Roithner LaserTechnik GmbH, Germany), and 405 nm laser (Thorlabs Ltd., UK). A 10× objective and 100 mm focal length lens images the FIG's proximal end onto a spectrograph slit (ImSpector, Spectral Imaging Ltd., Finland), which disperses the light onto an sCMOS camera (optiMOS; QImaging, Inc., Canada).

The image was scanned across the slit using a 1D scanning mirror (Thorlabs Ltd., UK) with the camera collecting an x-λ image at each mirror position. The start- and end-points of the scanning mirror were set so that the entire active area of the FIG was captured, and the step size set according to the number of lines required in the final reconstructed image. Raw x-λ images were used to reconstruct a stack of spectrally-resolved x-y images by integrating the signal over a user-defined bandwidth (10 nm) in the λ dimension. Positioning the mirror perpendicular to the spectrograph's optical axis allowed light to pass to an RGB camera (Prosilica; Allied Vision Technologies, USA) for navigation.

The system was tested on standard targets to characterise its spectral and spatial resolution (Macbeth colour chart and USAF target, respectively), field-of-view (FOV), and acquisition speed. It was then trialled in a porcine open abdominal surgical procedure to image the bowel serosal surface. The reconstructed stack of x-y images was used to generate an RGB image, extract the reflectance spectra of regions of interest, calculate tissue oxygen saturation (StO_2) [7], and collect autofluorescence emission under 375 and 405 nm excitation.

3. Results

Images of a USAF target at two different working distances are shown in Fig. 2 along with snapshots of the same FOV taken by the RGB navigation camera. At a working distance of 10 mm the FOV is 8 mm, with the Group 1, Element 4 lines resolvable. At 20 mm the FOV increases to 15 mm, while spatial resolution decreases. The Group 1, Element 4 lines parallel to the x-axis appear to be resolvable, while those parallel to the y-axis are indistinguishable.

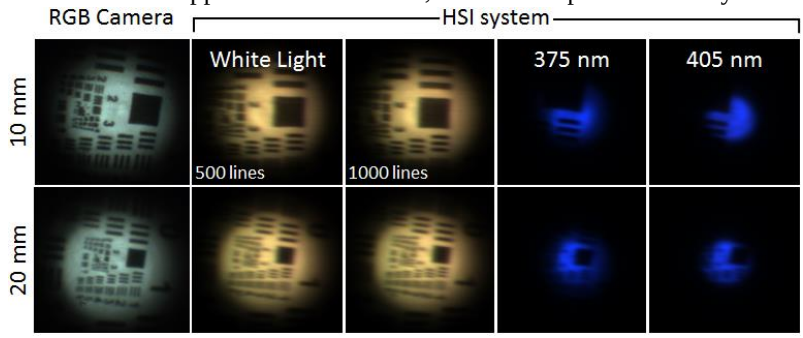

Fig. 2. Spatial resolution of the hyperspectral imaging system under three illumination conditions at two different working distances. The RGB images were captured using the RGB navigation camera.

System spectral resolution was quantified using the Macbeth colour chart. Normalised reflectance spectra of selected panels are shown in Fig. 3. While some qualitative differences between RGB and reconstructed colour images are apparent the recorded spectra show good agreement with those measured using a high resolution spectrometer (USB4000, Ocean Optics, Inc., USA). Areas of greatest deviation occurred below 450 nm and above 650 nm.

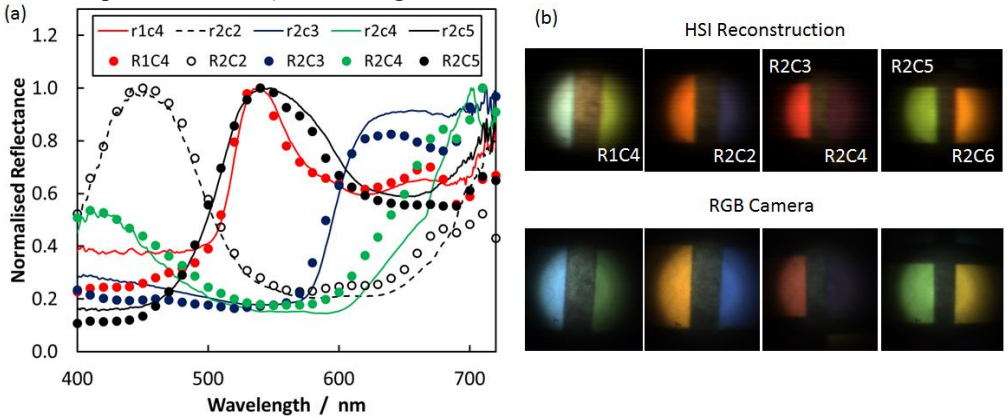

Fig. 3. (a) Normalised reflectance of Macbeth colour chart panels as measured by the HSI system (points), plotted on the same axes as spectra measured using a high-resolution spectrometer (lines). The legend indicates the row (r/R) and column (c/C) of the colour panel of interest (uppercase letters refer to the HSI system). (b) Colour images reconstructed from the hyperspectral stack are shown against those captured by the RGB navigation camera.

Initial *in vivo* results are shown in Fig. 4. Autofluorescence emission images were obtained by integrating the signal acquired at wavelengths greater than 450 nm. A characteristic broad spectrum is recorded for both excitation wavelengths (Fig. 4 (c)), with greater emission strength at 375 nm excitation. A colour image, Fig. 4 (d), reconstructed from 50 scan lines, shows small blood vessels (<1 mm diameter) on the tissue surface. To minimise breathing-related motion artefacts 4×4 pixel binning and a 50 ms exposure time were used. This resulted in a scan time of approximately 3 s for each acquisition. The absorbance spectra (Fig. 4 (c)), obtained under white light illumination from two regions of interest, display the distinctive haemoglobin features, with spatial variations in shape. The recorded absorbance spectra were used to calculate a map of oxygen saturation using linear regression (Fig. 4 (e)) [7].

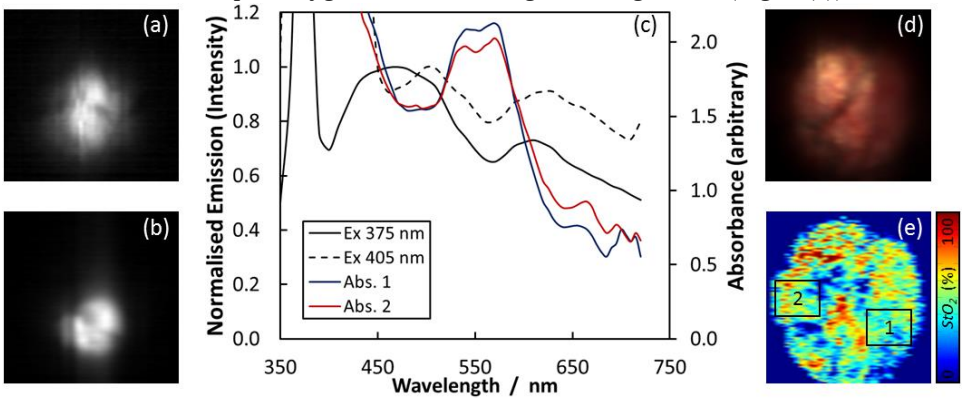

Fig. 4. Porcine small bowel imaging. Autofluorescence emission at (a) 375 nm excitation and (b) 405 nm excitation. (c) Normalised emission spectra (black lines) averaged over the areas in (a) and (b), as well as absorbance spectra from regions labelled in (e). (d) Colour image of tissue reconstructed from HSI data. (e) Oxygen saturation (StO_2) map of the serosa.

4. Conclusions

A dual white light reflectance and dual excitation autofluorescence hyperspectral imaging system has been demonstrated. The probe is small enough to fit within the instrument channel of a standard flexible endoscope and has a field-of-view of approximately 15 mm at a 20 mm working distance. *In vivo* results show that vascular features on the tissue surface were still resolvable despite breathing motion during the 3 s scanning time, and that reconstructed colour images of just 50 lines were qualitatively similar to high resolution RGB snapshot camera images of the same field. The system accurately reproduced the reflectance spectra of standard targets, as well as allowing recovery of oxygen saturation information from tissue data. Autofluorescence images and spectra were also recorded, with relative signal strength significantly stronger at 375 nm excitation.

5. Acknowledgements

Funding for this work was provided by an Imperial College Junior Research Fellowship (N. T. Clancy) and the National Institute for Health Research (NIHR) Biomedical Research Centre based at Imperial College Healthcare NHS Trust and Imperial College London. The authors would like to thank the Northwick Park Institute for Medical Research for their assistance with surgical arrangements.

6. References

[1] T. Kaltenbach, A. Rastogi, R. V. Rouse, K. R. McQuaid, T. Sato, A. Bansal, J. C. Kosek and R. Soetikno, "Real-time optical diagnosis for diminutive colorectal polyps using narrow-band imaging: the VALID randomised clinical trial," Gut (2014).

[2] L. B. Lovat, K. Johnson, G. D. Mackenzie, B. R. Clark, M. R. Novelli, S. Davies, M. O'Donovan, C. Selvasekar, S. M. Thorpe, D. Pickard, R. Fitzgerald, T. Fearn, I. Bigio and S. G. Bown, "Elastic scattering spectroscopy accurately detects high grade dysplasia and cancer in Barrett's oesophagus," Gut **55**, 1078-1083 (2006).

[3] A. Ignjatovic, J. E. East, T. Guenther, J. Hoare, J. Morris, K. Ragunath, A. Shonde, J. Simmons, N. Suzuki, S. Thomas-Gibson and B. P. Saunders, "What is the most reliable imaging modality for small colonic polyp characterization? Study of white-light, autofluorescence, and narrow-band imaging," Endoscopy **43**, 94-99 (2011).

[4] K. Imaizumi, Y. Harada, N. Wakabayashi, Y. Yamaoka, H. Konishi, P. Dai, H. Tanaka and T. Takamatsu, "Dual-wavelength excitation of mucosal autofluorescence for precise detection of diminutive colonic adenomas," Gastrointest. Endosc. **75**, 110-117 (2012).

[5] C.-C. Yu, C. Lau, G. O'Donoghue, J. Mirkovic, S. McGee, L. Galindo, A. Elackattu, E. Stier, G. Grillone, K. Badizadegan, R. R. Dasari and M. S. Feld, "Quantitative spectroscopic imaging for non-invasive early cancer detection," Opt. Express **16**, 16227-16239 (2008).

[6] G. Zonios, L. T. Perelman, V. Backman, R. Manoharan, M. Fitzmaurice, J. Van Dam and M. S. Feld, "Diffuse reflectance spectroscopy of human adenomatous colon polyps *in vivo*," Appl. Opt. **38**, 6628-6637 (1999).

[7] N. T. Clancy, S. Arya, D. Stoyanov, M. Singh, G. B. Hanna and D. S. Elson, "Intraoperative measurement of bowel oxygen saturation using a multispectral imaging laparoscope," Biomed. Opt. Express **6**, 4179-4190 (2015).